Dynamics of Biomolecules in Complex Microscale Geometries

Petr Hotmar

Department of Chemical and Biomedical Engineering
Florida State University

Dissertation Proposal Defense

April 21, 2010

Outline

- Motivation
- Model
- Results
- Future Work

Outline

- Motivation
- Model
- Results
- Future Work

Outline

- Motivation
- Model
- Results
- Future Work

Outline

- Motivation
- Model
- Results
- Future Work

Outline

- Motivation
- Model
- Results
- Future Work

Motivation

- Fundamental: biomolecules in electrokinetic flows under confinement in non-trivial geometries
- Application: lab-on-a-chip technologies, design and optimization

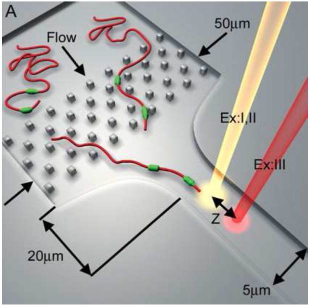

Direct Linear Analysis, developed by US Genomics. Source: [1]

Problem statement

- HYBRID MODEL; SOLVENT: isothermal, Newtonian, low *Re* limit on overlapping, structured, FD grids
- BIOMOLECULES: modified Langevin system subject to application dependent forces
- COUPLING: a semi-empirical hydrodynamic force, interpolation between lattice and off-lattice points

Objective

Model dynamics of biomolecules under electric fields while accounting for hydrodynamic interactions, thermal fluctuations in the fluid and non-linear electrokinetics.

Alternatives: Brownian / Stokesian dynamics, Lattice-Boltzmann, Dissipative particle dynamics, Stochastic rotation dynamics

Outline

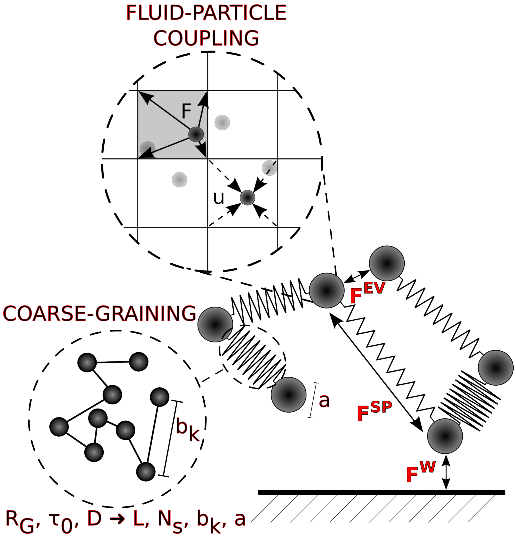
FLUID-PARTICLE COUPLING
F
u
COARSE-GRAINING
b_k
a
F^{EV}
F^{SP}
F^{W}
R_G, τ_0, D → L, N_s, b_k, a

Hydrodynamic forces

Newton's equations of motion

$$\frac{d\mathbf{r}_i}{dt} = \mathbf{v}_i,$$

$$m\frac{d\mathbf{v}_i}{dt} = \underbrace{-\zeta\left[\mathbf{v}_i(t) - \mathbf{U}(\mathbf{r}_i, t)\right] + \mathbf{F}_i^B(t)}_{\mathbf{F}_i^H(t)} \quad + \quad \underbrace{\mathbf{F}_i^{NH}(t),}_{\mathbf{F}^{SP}+\mathbf{F}^{EV}+\mathbf{F}^{W}\left(+\mathbf{F}^{EP}+\mathbf{F}^{DEP}\right)}$$

where fluctuation-dissipation theorem (FDT) requires

$$\left\langle F^B(t)\right\rangle = 0, \quad \left\langle F^B(t)F^B(t')\right\rangle = 2k_bT\zeta\delta(t-t').$$

$\mathbf{F}^B(t)$ is then

$$\mathbf{F}^B(t) = \left(\frac{6k_bT\zeta}{dt}\right)^{0.5} \cdot \mathbf{n}(t).$$

Non-hydrodynamic forces

The bonded force is modeled by the Marko-Siggia spring law (developed for semi-rigid worm-like chains such as DNA),

$$\mathbf{F}_i^{SP} = \frac{k_b T}{2 b_k} \left(\left(1 - \frac{R_i}{q_0} \right)^{-2} - 1 + \frac{R_i}{q_0} \right) \mathbf{R}_i$$

and excluded volume interactions by soft, Öttinger's potential,

$$\hat{\mathbf{F}}_i^{EV} = - \sum_{\substack{j=1 \\ i \neq j}}^{N} \sqrt{3}\, z_{ev}\, \frac{9}{2} \exp\left(-\frac{3}{2} \hat{R}_{ij}^2 \right) \hat{\mathbf{R}}_{ij}.$$

The bead-wall repulsion is modeled by a potential suggested by Jendrejack [4], which yields

$$\mathbf{F}_i^{W} = \begin{cases} \frac{-A_w}{b_k\, \delta_w^2} \left(D_i - \delta_w \right)^2 \nabla D_i & \text{if } D_i < \delta_w \\ \mathbf{0} & \text{if } D_i \geq \delta_w. \end{cases}$$

Distance function

The normal distance to the nearest wall is found as the solution to the Eikonal equation

$$\begin{aligned} |\hat{\nabla}\hat{D}| &= 1 && \text{for } \mathbf{x} \in \Omega, \\ \hat{D} &= 0, && \text{for } \mathbf{x} \in \Gamma_W, \\ \hat{\nabla}\hat{D}\cdot\mathbf{n} &= 0, && \text{for } \mathbf{x} \in \Gamma_I \cup \Gamma_O. \end{aligned} \qquad (1)$$

Due to Neumann BCs, we convert Eq. (1) into

$$\frac{d\hat{D}}{d\hat{t}} = -\left(\hat{\nabla}\hat{D}\right)^2 + \gamma\,\hat{\Delta}\hat{D} + 1 \qquad \text{for } \mathbf{x} \in \Omega.$$

- Method of lines, Adams-Bashforth started with 4th order Runge-Kutta, stabilized with artificial diffusion
- Kd-tree and approximate nearest neighbor (ANN) search used for efficiency

Distance function in an entropic trap

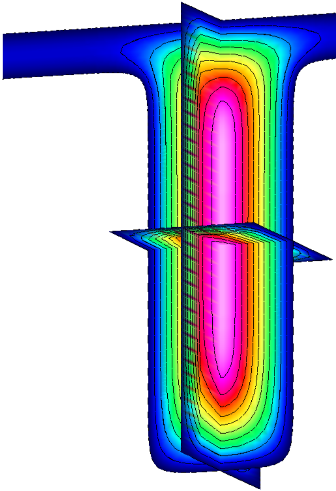

Electric field

- Potential split into intrinsic (EDL) and applied (external) contributions, $\phi = \phi_i + \phi_a$
- Needed for electrophoretic ($\propto \mathbf{E} = -\nabla\phi_a$) and dielectrophoretic ($\propto \nabla|\mathbf{E}|^2$) forces
- Debye-Hückel approximation, linearized Poisson-Boltzmann equation

$$\begin{aligned}
\hat{\nabla}^2\hat{\phi}_i &= \hat{\kappa}^2\hat{\phi}_i, && \text{for } \mathbf{x} \in \Omega,\\
\hat{\nabla}\hat{\phi}_i \cdot \mathbf{n} &= 0, && \text{for } \mathbf{x} \in \Gamma_I \cup \Gamma_O,\\
\hat{\phi}_i &= \hat{\zeta}_w, && \text{for } \mathbf{x} \in \Gamma_W,\\
\hat{\nabla}^2\hat{\phi}_a &= 0, && \text{for } \mathbf{x} \in \Omega,\\
\hat{\phi}_a &= \hat{\phi}_{max,app}, && \text{for } \mathbf{x} \in \Gamma_I \cup \Gamma_O,\\
\hat{\nabla}\hat{\phi}_a \cdot \mathbf{n} &= 0, && \text{for } \mathbf{x} \in \Gamma_W.
\end{aligned}$$

Intrinsic and applied potentials

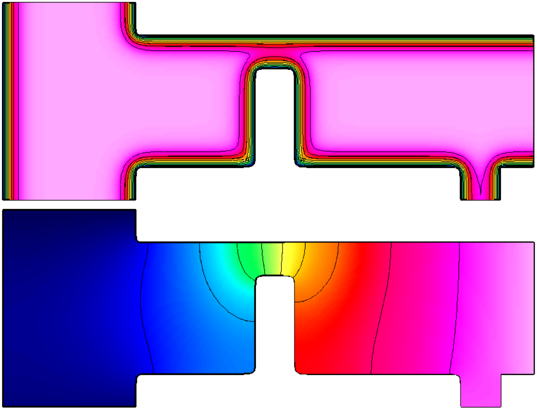

Intrinsic and applied potentials in the DEP device.

Unperturbed fluid velocity and pressure

- Primitive variables $(\hat{\mathbf{u}}, \hat{p})$ formulation with electric body force $\hat{\mathbf{f}}_\mathbf{e} = \hat{\kappa}^2 \hat{u}_{HS} \hat{\phi}_i \hat{\nabla} \hat{\phi}_a$, $Re \to 0$ yields Stokes flow
- Poisson equation for pressure (incompressibility included) with a penalty term $\alpha \nabla \cdot \mathbf{u}$ to damp out oscillations

$$
\begin{aligned}
\frac{\partial \boldsymbol{\Theta}}{\partial \tau} &= L\boldsymbol{\Theta} + G, && \text{for } \mathbf{x} \in \Omega, \\
\hat{\mathbf{u}} &= 0 \quad \text{(no slip)}, && \text{for } \mathbf{x} \in \Gamma_W, \\
\hat{\nabla}\hat{\mathbf{u}} \cdot \mathbf{n} &= 0 \quad \text{(free stream)}, && \text{for } \mathbf{x} \in \Gamma_I \cup \Gamma_O, \\
\frac{\partial \hat{p}}{\partial \mathbf{n}} &= -\mathbf{n} \cdot \nabla \times \nabla \times \hat{\mathbf{u}} + \mathbf{n} \cdot \hat{\mathbf{f}}_\mathbf{e}, && \text{for } \mathbf{x} \in \Gamma, \text{ where}
\end{aligned}
$$

$$
\boldsymbol{\Theta} = \begin{bmatrix} \hat{\mathbf{u}} \\ \hat{p} \end{bmatrix}, \quad L = \begin{bmatrix} \hat{\Delta} & -\hat{\nabla} \\ -\hat{\alpha}\hat{\nabla}\cdot & \hat{\Delta} \end{bmatrix}, \quad G = \begin{bmatrix} \hat{\mathbf{f}}_\mathbf{e} \\ -\hat{\nabla} \cdot \hat{\mathbf{f}}_\mathbf{e} \end{bmatrix}.
$$

Particle-fluid coupling and fluctuating hydrodynamics

$$\mathbf{f}_{tot}(\mathbf{r},t) = \mathbf{f}_e(\mathbf{r}) + \mathbf{f}_c(\mathbf{r},t) + \nabla \cdot \mathbf{S},$$

where the particle-fluid coupling is defined as

$$\mathbf{f}_c(\mathbf{r},t) = -\sum_{i=1}^{N} \left\{ \zeta_{eff} \left[\mathbf{U}(\mathbf{r}_i,t) - \mathbf{v}_i(t) \right] + \mathbf{F}_i^B(t) \right\} \delta(\mathbf{r}-\mathbf{r}_i),$$

and the Landau-Lifshitz stochastic flux tensor $\mathbf{S}$ has zero mean and covariance given by the FDT,

$$\left\langle \mathbf{S}_{ij}\left(\mathbf{r},t\right) \mathbf{S}_{kl}\left(\mathbf{r}',t'\right) \right\rangle = 2k_b T \eta \left(\delta_{ik}\delta_{jl} + \delta_{il}\delta_{jk} - \frac{2}{3}\delta_{ij}\delta_{kl} \right) \delta^{\mathbf{rr}'} \delta^{tt'},$$

Velocity disturbance near a plane wall

- Analytically: Blake's method of image singularities
- Formation of polymer depletion layers, increase in ζ and τ_0

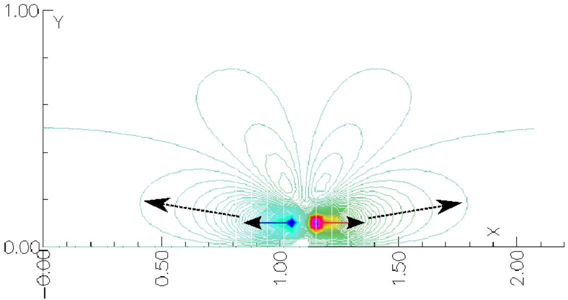

Velocity contour lines of a disturbance field due to force dipole.
Solid arrows - forces; dashed arrows - velocity vectors.

Histogram of COM in a confined channel

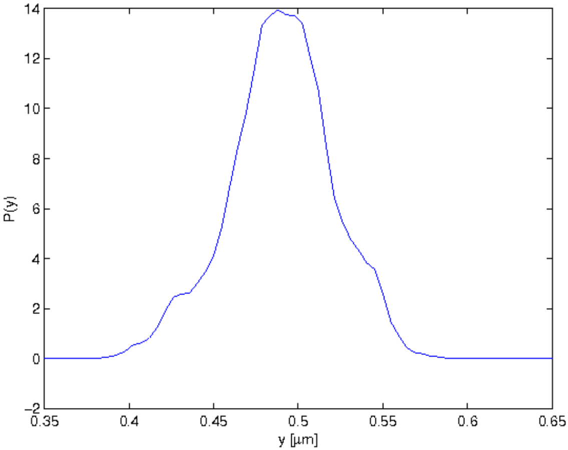

Decay of VAF, long-time tails, deterministic experiment

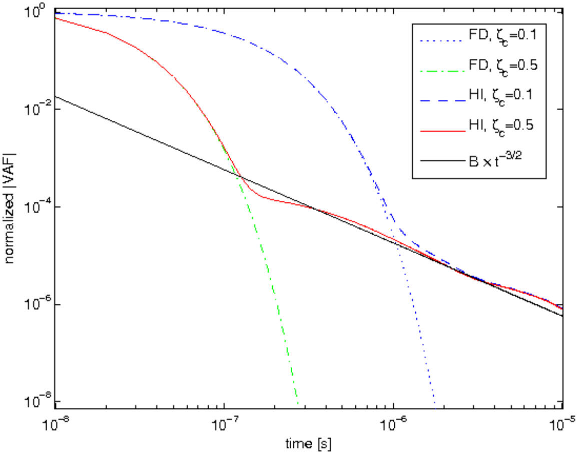

Thermal equilibrium, stochastic experiment

- FDT does not hold for reduced coupling $\mathbf{F}_i^{CPL}(\mathbf{r}_i, t) = -\zeta_{eff}\left[\mathbf{v}_i(t) - \mathbf{U}(\mathbf{r}_i, t)\right]$ in a fluctuating fluid.

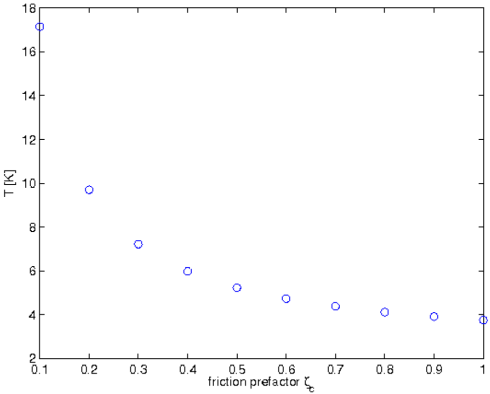

Stretch-coil transition, Time evolution of directional stretch

- τ_0 extracted from an exponential fit to the chain stretch, agrees with Fox-Flory prediction

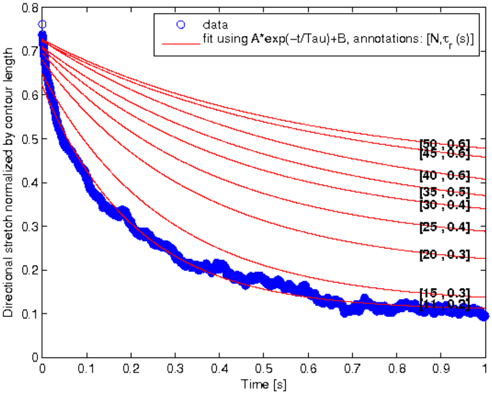

Relaxation time, scaling with N

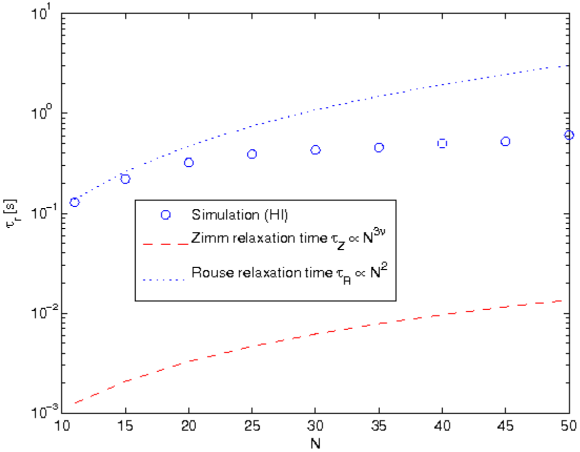

R_g scaling, FD simulation

- Initial conformation grown on a 3D lattice as a SARW
- $R_g^2 \equiv \frac{1}{N^2} \sum_{i=1}^{N} \sum_{j=i}^{N} (\mathbf{R}_i - \mathbf{R}_j)^2$

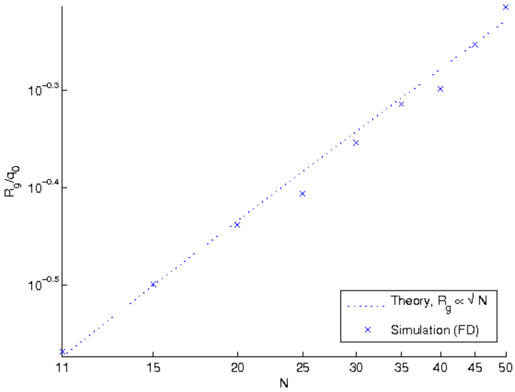

D scaling, HI simulation

- Diffusivity obtained from the Einstein formula, $D = \lim_{t\to\infty} \frac{\langle |\mathbf{r}(t) - \mathbf{r}(0)|^2 \rangle}{6t}$

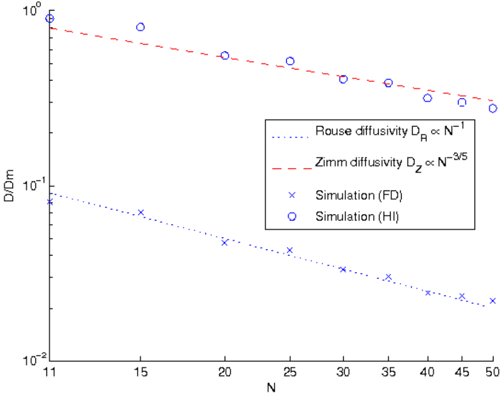

Outline

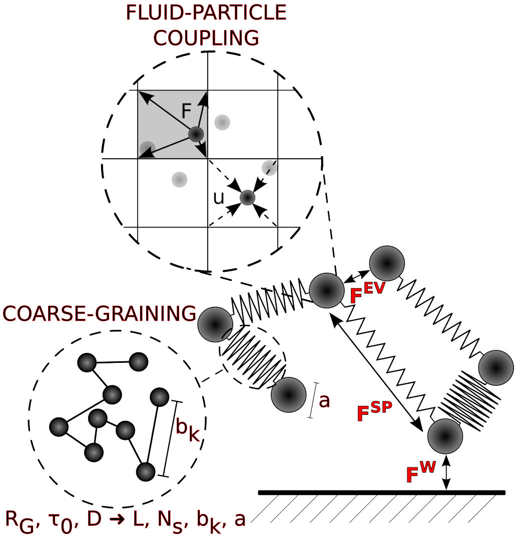
FLUID-PARTICLE COUPLING
F
u
COARSE-GRAINING
b_k
a
F^{EV}
F^{SP}
F^{W}
R_G, τ_0, D → L, N_S, b_k, a

Outline

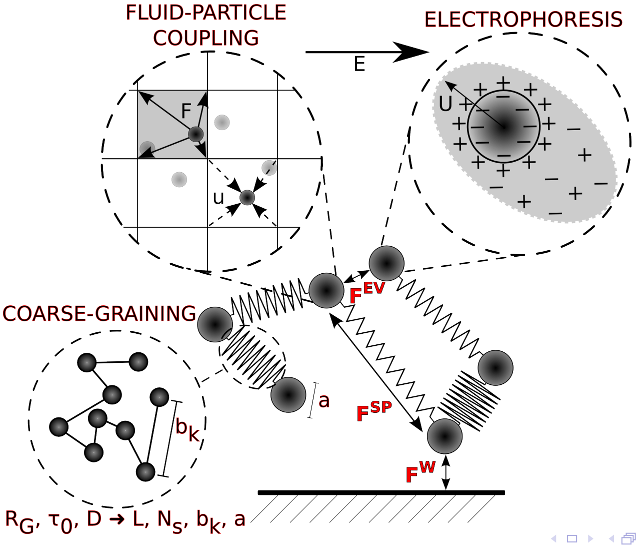
FLUID-PARTICLE COUPLING
ELECTROPHORESIS
E
F
u
U
COARSE-GRAINING
b_k
a
F^{EV}
F^{SP}
F^{W}
R_G, τ_0, D → L, N_s, b_k, a

Entropic trapping, theory

- EP separation: free-solution vs gel vs “artificial” gel [3]
- Long molecules will travel faster than the short ones!

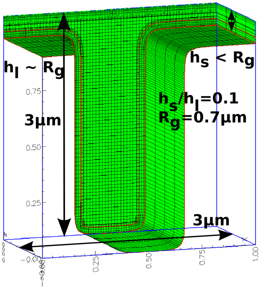

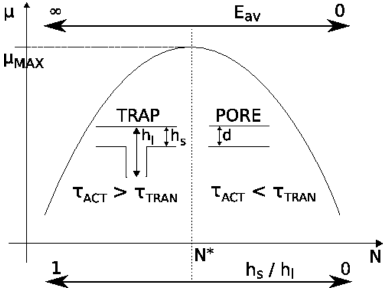

$$\tau_{trap} \sim \tau_0 \exp(\Delta F), \quad \Delta F \sim m - E_s m^2, \quad \tau_0 \sim N^{-\nu} D^{-1}$$

Entropic trapping, simulations

- HIs neglected
- Charge screening due to counter-ion condensation. Using Rouse model and experimental μ_0, we estimate $Q_{eff} = \mu_0 6\pi\eta a = 270\ e \Rightarrow$ screening $= 24\ \%$

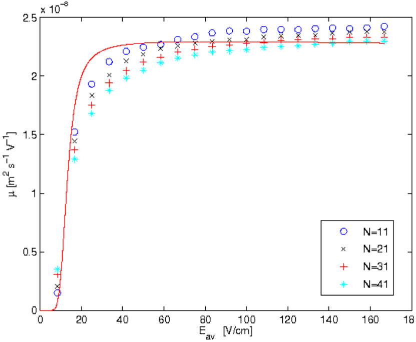

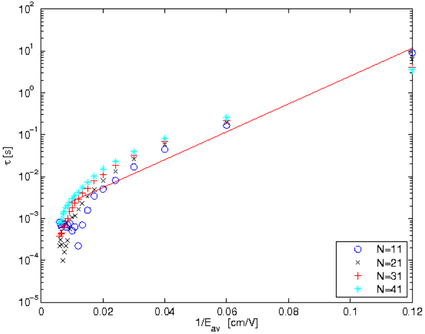

Entropic trapping, predictions

- Limiting behaviors of μ observed for $E = 8.3$ V/cm and $E = 25$ V/cm. The maximum occurs for $E \sim 12$ V/cm.

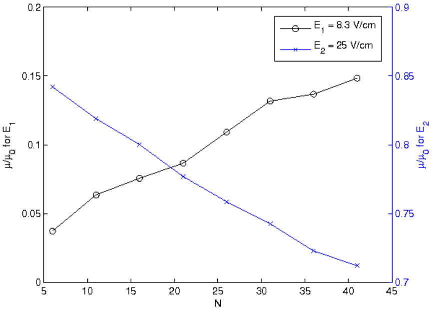

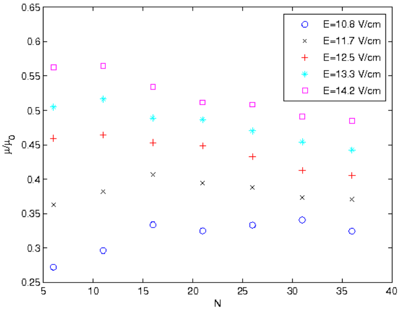

Trapping, animation

Migration of short (N=11) and long (N=41) chains. While the long chain successfully migrates, short chain is mostly governed by isotropic diffusion.

Kang's dielectrophoretic (DEP) separator

- Kang's DEP separator [2], EP + DEP forces
- Separation based on size and/or polarizability,
  $\mathbf{F}_{DEP} = (\mathbf{p}_{eff} \cdot \nabla)\,\mathbf{E} = 2\pi\epsilon_f a^3 K_{CM} \cdot \nabla|\mathbf{E}|^2$.

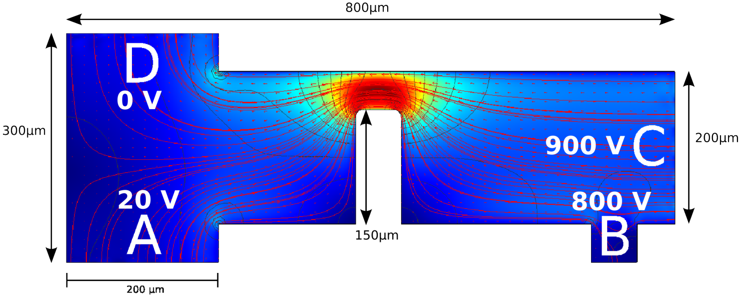

- Simulations (inertial, 3D, F^B, f_e) found sensitive to the neglect of particle inertia and dimensionality reduction

Quadrupolar correction to DEP force

Kang et al. introduce a heuristic factor c to correct for finite-size of particles. To quantify, we use multipolar expansion of DEP force

$$\mathbf{F}_{DEP}^{(n)} = \frac{4\pi\epsilon_f a^{2n+1}}{(n-1)!\,(2n-1)!!} K_{CM}^{(n)} (\nabla)^{n-1}\mathbf{E}[\cdot]^n(\nabla)^n\mathbf{E},$$

where $(2n-1)!! \equiv (2n-1)\cdot(2n-3)\cdot\ldots\cdot 5\cdot 3\cdot 1$ and $[\cdot]^n$ means n dyadic multiplications. The first two terms of the i-th component of the force, dipole and quadrupole, are then

$$(F_{DEP})_i = 4\pi\epsilon_f a^3 \left\{ -\frac{1}{2}E_m\frac{\partial E_i}{\partial x_m} - \frac{1}{9}a^2 E_m \frac{\partial E_n}{\partial x_m}\frac{\partial^2 E_i}{\partial x_n \partial x_m} - \ldots \right\}.$$

We found $c_Q \equiv F^{(2)}/F^{(1)}$ to be about 10%. Since c reported $\sim$ 60-70%, other contributions should be identified.

Separation, animation

DEP separation of 5μm (blue) and 15μm (green) particles.

Outline

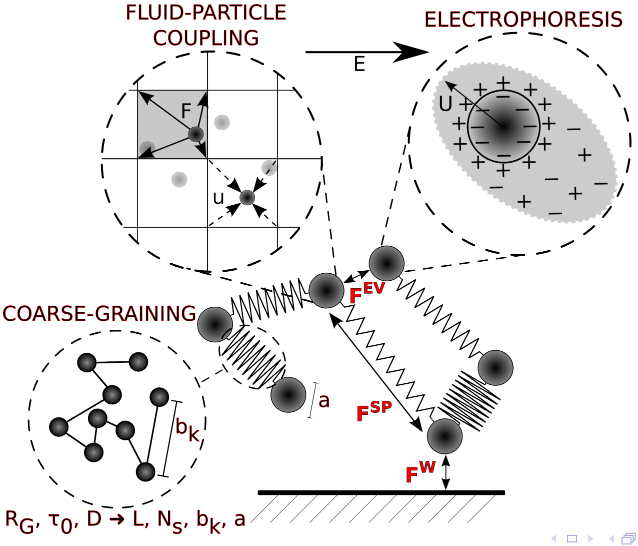
FLUID-PARTICLE COUPLING
F
u
E
ELECTROPHORESIS
U
COARSE-GRAINING
b_k
a
F^{EV}
F^{SP}
F^{W}
$R_G, \tau_0, D \rightarrow L, N_S, b_k, a$

Outline

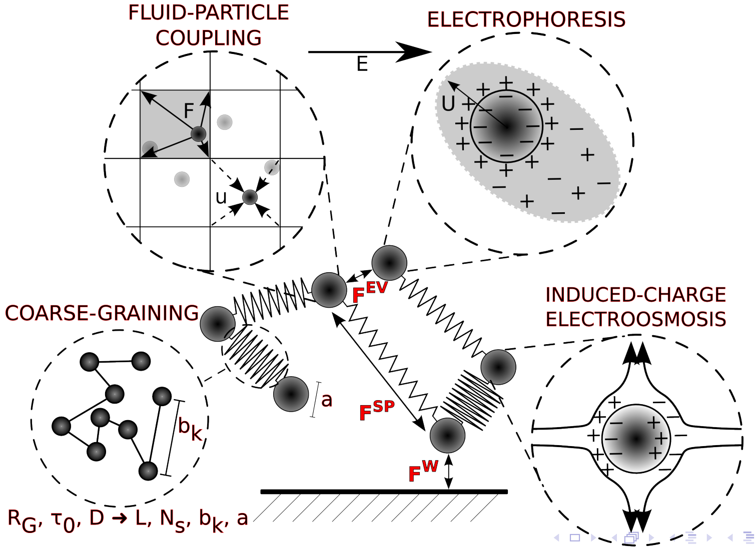
FLUID-PARTICLE COUPLING
F
u
E
ELECTROPHORESIS
U
COARSE-GRAINING
a
F^{EV}
F^{SP}
F^{W}
INDUCED-CHARGE ELECTROOSMOSIS
b_k
R_G, τ_0, D → L, N_S, b_k, a

Induced-charge electro-osmosis (ICEO) around sharp corner

- ICEO = non-linear flows arising from interactions of the external field with non-uniform EDLs induced by the same field
- Charge spatially varying, generates dipolar charge cloud which then drives a "quadrupolar" ICEO flow
- ICEO flow around the obstacle of the DEP separator

BC $\hat{\phi}_i = \hat{\zeta}_w$ for $\mathbf{x} \in \Gamma_W$ modified as follows:

$$\hat{\phi}_i(\mathbf{x}) = \hat{\zeta}_w - \hat{\phi}_a(\mathbf{x}) + \hat{\phi}_c, \qquad \text{for } \mathbf{x} \in \Gamma_o,$$

where the correction potential $\hat{\phi}_c$ is introduced to ensure neutrality,

$$\frac{1}{\Gamma_o}\int_{\Gamma_o} \hat{\phi}_i(\mathbf{x}) d\Gamma_o = \hat{\zeta}_w, \quad \text{i.e. } \hat{\phi}_c = \frac{1}{\Gamma_o}\int_{\Gamma_o} \hat{\phi}_a(\mathbf{x}) d\Gamma_o.$$

ICEO, cont'd

EDL surface potential $\hat{\phi}_i$ around the obstacle. The ICEO velocity (red vector field) indicates a weak vortex flow.

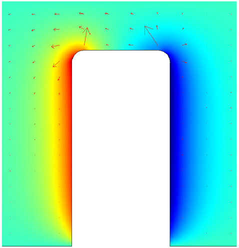

- Found negligible effect on separation efficiency. It is reasonable to expect, however, that the ICEO flow arising due to particle polarizability and mediated by HIs may no longer be negligible.

Counterion analysis in traps and separators, shape optimization

- Counterions sheared away in confinement. Non-monotonic dependence of μ on N due to the competition between HIs and charge screening reported in bulk.
- We expect disappearance of the maximum in the mobility curve.
- Shape optimization of insulating obstacles to improve selectivity/efficiency. applications: DNA tagging and sequencing, DNA translocation in ion channels and synthetic nanopores.

Extensional flows in a hyperbolic die

- Extensional flows (EFs) can be sustained over a relatively large region, as opposed to localized EFs in four-roll mills.
- Efficiency of electric-field-driven stretching in a hyperbolic die

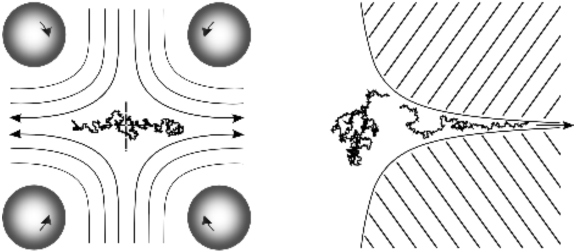

Four-roll mill (left) and hyperbolic die (right).

Frictional coupling in "raspberry" colloids

- Extension of particle-fluid coupling to bead-spring networks, capable of representing colloids
- Shown to recover VAF tails, various surfaces may be modelled
- Would be applied to the DEP device and studied in both dilute and dense suspensions.
- Deficiency: loss of accuracy in colloids near contact → lubrication corrections?

IBM-like electrostatics

- Include electric field perturbation due to particle presence in polymer dynamics and/or ICEO flows around moving particle
- Account for similarly to the frictional coupling and Immersed Boundary Method (IBM) approaches of hydrodynamics to avoid expensive re-meshing
- The source term in the governing equation would be modified to reproduce the effect of boundary conditions.
- The applied (similarly intrinsic) potential would then be governed by

$$\nabla \cdot (\epsilon_f \nabla \phi) + S = 0, \qquad \text{for } \mathbf{x} \in \Omega,$$

where

$$S = \begin{cases} \nabla \cdot ((\epsilon_p - \epsilon_f) \nabla \phi_P) & \text{for } \mathbf{x} \in \Omega_P, \\ 0 & \text{for } \mathbf{x} \in \Omega \setminus \Omega_P, \end{cases} \qquad (2)$$

References / Questions

- E. Y. Chan, N. M. Goncalves, R. A. Haeusler, A. J. Hatch, J. W. Larson, A. M. Maletta, G. R. Yantz, E. D. Carstea, M. Fuchs, G. G. Wong, S. R. Gullans, and R. Gilmanshin, *DNA mapping using microfluidic stretching and single-molecule detection of fluorescent site-specific tags*, Genome Res. (2004).
- K. H. Kang et al., *Continuous separation of microparticles by size with direct current-dielectrophoresis*, Electrophoresis (2006).
- J. Han and H. G. Craighead, *Characterization and optimization of an entropic trap for DNA separation*, Anal. Chem. (2002).
- R. M. Jendrejack and D. C. Schwartz, *Effect of confinement on DNA dynamics in microfluidic devices*, J. Chem. Phys. (2003).